# Potential-Induced Wetting and Dewetting in Hydrophobic Nanochannels for Mass Transport Control

Seol Baek <sup>1†</sup> , Seu	ing-Ryong Kwor	1 <sup>2†</sup> , and Paul Y	W. Bohn <sup>1,3*</sup>
-------------------------------	----------------	------------------------------	-------------------------

<sup>1</sup>Department of Chemistry and Biochemistry, University of Notre Dame, Notre Dame, Indiana 46556, United States

<sup>2</sup>Department of Chemistry and Research Institute of Natural Science, Gyeongsang National University, Jinju, 52828, South Korea

<sup>3</sup>Department of Chemical and Biomolecular Engineering, University of Notre Dame, Notre Dame, Indiana 46556, United States

<sup>†</sup>Seol Baek and Seung-Ryong Kwon contributed equally to this work.

<sup>\*</sup>Author to whom correspondence should be addressed, *pbohn@nd.edu* 

### **Abstract**

Wetting and dewetting transitions play a central role in controlling the hydrophobicity of the lining of biological channels in order to regulate aqueous solution permeation. Understanding of the operational characteristics of biological nanochannels led to experimental efforts to mimic their behavior and to achieve potential-induced, repeatedly-switchable wettability transitions in synthetic nanochannels in the early 2010s. Since then, research has identified conditions needed to produce reversible wettability transitions using a number of different environmental stimuli - such as light, pH, and electrostatic charge - in addition to potential. Furthermore, nascent understanding of the underlying phenomena in synthetic nanochannels was rapidly followed by practical applications, including oil-water separations, drug release, and electroactive flow control based on switchable wettability. More practical applications are being developed continuously, as the physical and chemical principles that govern hydrophobic gating at the nanoscale are further elucidated, making it possible to exploit wettability as a design element in nanofluidic systems.

# **Keywords**

Electrowetting, mass transport, nanochannel, hydrophobicity, wettability

# Introduction

In biological membranes, ion channels make it possible to realize rapid and efficient, ion-specific transport across the membrane. Typical ion channels exhibit an internal diameter ~1 nm, a structural characteristic that plays a key role in achieving selective transport of ions and facilitates their ability to modulate mass transport by wetting and dewetting transitions [1]. Typically, when a pore is in its dewetted state, a vapor barrier is formed, which blocks the

permeation of aqueous solution and the accompanying transport of ionic and neutral solutes. However, wetting is accompanied by a vapor-to-liquid phase transition, filling the nanochannels with aqueous solution, thereby enabling ion permeation [2-4]. In the dewettedto-wetted transition, a potential gradient of 50 - 200 mV develops across the biological membrane, which facilitates hydration of the lining of the pore [5], thereby making it possible for aqueous solution to pass, effectively opening the closed gate to solution transport, as shown schematically in Figure 1A. Inspired by the effective transport control obtained through wetting and dewetting transitions in the hydrophobic lining of biological ion channels, considerable recent attention has been paid to the use of wettability transitions in synthetic nanochannels as a route to producing externally-controllable biomimetic channels, with the goal of using them in technological applications, such as micro/nanofluidic valves for controlled transport and fluidic gating, water treatment/separation, and energy conversion [6-8]. In the effort to mimic the transport control functions of biological nanopores, solid-state nanopores have emerged as a promising alternative because of their robustness to structural damage, tunable pore sizes, e.g., diameter and length, and the availability of straightforward routes to molecular decoration of the pore surface in order to achieve engineered ion/molecular transport specificity [9, 10].

One of the greatest challenges to exploiting biomimetic wettability transitions to engineer smart channels is fabricating sub-nanometer channels (or pores) commensurate in size with biological nanochannels. Size is important in this context, because small channels facilitate efficient interactions of the permeant molecules with the pore lining. Nuclear particle damage track-etching and focused ion-beam milling have been successfully applied to the fabrication of conically shaped nanochannels with a large opening at one end and a smaller opening - down to a few 10s of nanometers - at the other end [11-17]. However, these methods are not capable of producing pores with diameters < 5 nm, comparable to the size of biological *Potential-Induced Wetting and Dewetting in Hydrophobic Nanochannels.....* 

nanochannels. One approach to resolving the small pore fabrication problem involves manufacturing high aspect-ratio nanochannels with a large (μm-scale) channel length and a pore opening diameter of a few 10s of nanometers. For example, Siwy and coworkers fabricated a 12 μm long channel with a ~30 nm pore opening in a polyethylene terephthalate film, and ensured the hydrophobicity of the inner channel surface by chemical functionalization [18]. In an alternative approach, Tabard-Cossa and coworkers recently developed a method for single nanopore fabrication, capable of producing nanopores down to ~2 nm pore diameter using controlled dielectric breakdown of thin silicon nitride (SiN<sub>x</sub>) membranes [19]. Even sub-nm nanopores have been prepared by other groups in order to achieve fast water transport using carbon nanotube (CNT) porins with ~0.8 nm diameter [20].

Another challenge focuses on ensuring that the wettability transitions on the inner nanochannel surfaces are reversible. Initial efforts to engineer reversible surface characteristics used light- or pH-responsive hydrophobic-to-hydrophilic (or *vice-versa*) switchable molecules to immobilized on the nanochannel surface [21-23]. However, these types of hydrophobic-to-hydrophilic transitions are typically accompanied by molecular structural changes that are not reversible in many cases, frequently because the reverse transition is not kinetically favorable. Thus, instead of exploiting direct molecular conformational changes to effect wettability transitions in nanopores, an alternative approach employing potential-induced wetting and dewetting in hydrophobic pores has recently attracted significant attention. This strategy is motivated by the hydrophobic gating in biological ion channels as well as predictions from simulations, **Figure 1B** [5, 6, 24, 25]. In the early 2010s, the Smirnov and Siwy groups experimentally demonstrated reversible wetting and dewetting in hydrophobic nanopores controlled by external potentials, showing high and low (or zero) conductance, as shown in **Figure 1C** [18, 26, 27]. Inspired by these earlier experimental observations, multiple stimuli -

light, electrostatic charges, pH, and potential - have been explored either singly or in combination to induce wettability transitions [28-31]. In this Opinion, we will review recent work focusing on potential-induced and multiple stimuli-induced switchable wetting and dewetting in hydrophobic nanochannels. The current mechanistic understanding and evidence supporting it will be covered, and some initial applications exploiting wettability transitions will be also described.

At the outset, it is important to distinguish the effects of applied potential with those attributed to electric field. Commonly, the two effects are convoluted. The primary independent variable, however, is potential, and whether it is potential directly or the electric fields which are established as a result of the application of a bias voltage depends on details of the structure and experimental protocol. Ascribing wetting/dewetting phenomena to electric fields assumes a detailed understanding of the spatial and temporal characteristics of potential distributions in the nanoscale architectures interest. This information is often difficult to acquire, so for the purposes of this review, we will describe the effects to potential, while understanding that some behaviors may more appropriately be attributed to the resulting electric field and its distribution in space and time.

# Wetting and dewetting in hydrophobic nanopores

Fluidic behavior in confined nanochannels deviates significantly from behavior in larger structures, in particular being dominated by physicochemical interactions between the permeating liquid and the nanochannel surface [32-35]. In hydrophobic nanochannels, spontaneous dewetting occurs due to minimized interactions between polar water molecules and nonpolar wall surfaces as compared to water interactions with hydrophilic surfaces, leading to enhanced water evaporation and minimizing contact of water molecules with the *Potential-Induced Wetting and Dewetting in Hydrophobic Nanochannels.....* 5

hydrophobic surface. The presence of a vapor in the hydrophobic lining of the nanochannel increases the free energy barrier for molecular transport, preventing water and solute permeation through the nanopores. Thus, introducing and controlling the hydrophobicity of the inner pore surface along the nanochannel is a crucial factor in realizing reversible wetting and dewetting. For example, the presence of an extended vapor in a hydrophobic nanochannel with a small pore diameter ( $d \sim 20$  nm) makes it difficult to achieve potential-induced wetting of the nanochannel due to the high free energy barrier presented [18]. In contrast, small isolated hydrophobic clusters along the channel, produced by chemical functionalization, can provide an adequate free energy barrier to enable reversibly switchable wetting/dewetting transitions that can be controlled by potential [26]. Near the wetted-dewetted transition small fluctuations in conditions can produce large fluctuations in local hydrophobicity giving rise to apparently random transitions between wetted and dewetted states. Stochastic liquid-vapor transitions have been observed by molecular dynamics (MD) simulations of model nanopores [36], and numerous computational and theoretical studies have reported on the detailed mechanism of wetting/dewetting under hydrophobic confinement [37-43].

An attractive strategy to realize reversibly-controllable wetting and dewetting in hydrophobic nanochannels, involves applying electric potentials to induce nanochannel wetting/dewetting transitions, *i.e.*, electrowetting [44, 45]. Several possible mechanisms have been proposed to explain the detailed functioning of potential-induced wetting and dewetting in hydrophobic nanochannels. In one model, the three-phase contact lines are pinned, but the changing shape of the liquid-vapor interface induces the menisci to overlap. This shape change results from the electrostatic attraction of oppositely charged ions in opposing menisci facing one another across the vapor gap. In a second model, the liquid contact angle on the channel wall changes, and the contact lines move under electrostatic pressure [27]. Electrophysiology simulations have characterized the influence of applied electric potentials on the wetting of a *Potential-Induced Wetting and Dewetting in Hydrophobic Nanochannels.....* 

hydrophobic gate in a model β-barrel membrane protein nanopore, showing that voltage-induced alignment of water dipoles within the hydrophobic region lowers the energy for water entry, which is accompanied by ion permeation [46]. Potential-controlled water transport has been also examined by MD simulations in graphene nanochannels and interpreted to result from water dipole reorientation in response to the spatiotemporal potential and asymmetric charge density distributions [47]. More recently, Klesse and coworkers have investigated the effect of a transmembrane voltage on hydrophobic pore wetting in a model protein nanopore derived from the 5-HT<sub>3</sub> receptor using MD simulations, and found that the threshold voltage to induce wetting depends on the orientation of the electric-field generated by the distribution of charged amino acids on the pore lining [5].

# Potential-induced wetting and dewetting of nanochannels

A diverse variety of artificial, solid-state nanopores have been fabricated for direct experimental observation of wetting and dewetting transitions. Smirnov and coworkers prepared 60-600 nm diameter nanopores rendered hydrophobic by modification with trimethoxyhexadecylsilane ((MeO)<sub>3</sub>SiC<sub>16</sub>H<sub>33</sub>) in 300 nm-thick SiN<sub>x</sub> membranes, and observed transitions between two distinct states, a dry low conductance state and a wet high conductance state. The two states exhibited greater than  $10^3$ -fold difference in conductance upon applying and releasing a bias voltage [27]. The reversibility of wetting/dewetting transitions was observed to depend on geometry (pore diameter) and applied potential, with the transitions being irreversible for larger diameter pores ( $d \ge 300$  nm) and bias voltages exceeding a sample-dependent threshold. Siwy and coworkers, used longer nanopores prepared in 12 µm-thick polyethylene terephthalate films to achieve reversible wetting and dewetting transitions between states showing high and near-zero conductance, respectively, in single hydrophobic

nanopores [18]. The conically shaped nanopore (16 nm diameter at the small opening) was modified with (trimethylsilyl)diazomethane to create local hydrophobic areas, where water vapor is formed more readily, thus blocking the flow of water and ions, and the potential-dependent hydrophobic gating response was characterized by the ionic current passing through the single nanopore. The ionic current was observed to fluctuate between high and low conductance states suggesting that reversible wetting and dewetting processes are associated with dynamic water condensation and evaporation processes inside the nanopore.

The same group studied the influence of electrolyte concentration on wetting and dewetting behavior in single polymer-embedded nanopores in which the surfaces were modified with alkyl chains of different length, i.e.,  $C_3 - C_{10}$  chains, as a function of increasing ionic strength, i.e., 10 mM – 1 M KCl [48]. At low (10 mM KCl) ionic strength, the nanopores with short alkyl chains exhibited a weak hydrophobic gating response, predominantly remaining in the conductive state in a voltage range of -10 V.  $< E_{appl} < +10$  V. However, hydrophobic nanopores modified with longer alkyl chains showed almost no conductance over the entire voltage range at low ionic strength, while potential-induced wetting and dewetting was facilitated at higher ionic strengths. These observations were explained by a combination of Maxwell stress and osmotic pressure accompanying the shape change of the meniscus at the water-vapor interface. Later, electrowetting-induced enhancements in ion transport rate were demonstrated using 14 nm diameter CNTs, by decreasing the interfacial tension between the interior nanopore surfaces and water, thereby promoting the formation of water channels inside the CNT [49]. Very recently, the dependence of hydrophobic gating on the size and hydration strength of various solvated anions - chloride (Cl<sup>-</sup>), bromide (Br<sup>-</sup>), and iodide (I<sup>-</sup>) - was explored in SiN<sub>x</sub> nanopores containing a hydrophobic-hydrophilic junction, Figure 2A [50]. Solutions containing large anions, such as Br and I , showed enhanced electrowetting in the pores, which was attributed to anion accumulation at the hydrophobic surface due to the weaker Potential-Induced Wetting and Dewetting in Hydrophobic Nanochannels.... 8

solvation shell of the large polarizable ions, as shown in Figure 2B. Similarly, Bohn and coworkers reported electrowetting-mediated mass transport in small defect nanochannels in SiN<sub>x</sub> gate dielectrics within 3-electrode embedded nanopore electrode arrays, Figure 2C,D [23]. The strong electrowetting and dewetting behavior in the defect nanochannels was used to control redox species transport across the defects and then combined with redox cycling between separate annular electrodes in the vestibule of the NEA nanopores. As a result, electrochemical transistor operation was achieved with the rectification factor of ~440 by manipulating electric-field-induced wetting and dewetting, as shown in Figure 2C.

# Multiple external stimuli-controlled wetting and dewetting of nanochannels

In addition to potential-induced wettability gating, multiple other external stimuli, e.g., pH, light, temperature, and host-guest chemistry, have been used to effect wetting and dewetting and mimic the behavior of biological channels as well as provide the basis for a range of practical applications. As one example, Jiang and coworkers reported electrostaticcharge- and electric-field-induced gating of nanochannel transport by regulating the surface charge density and applied external bias [28]. These researchers later designed azobenzene derivative (Azo)-functionalized hydrophobic polymer nanochannels to regulate mass transport employing light- and electric field-controlled wetting behavior [29]. In their work, lightinduced wetting/dewetting behavior was based on altering the structure and composition of host-guest complexes, as shown in Figure 3A.

In addition, ion transport regulated by hydrophobic domains has been investigated in response to dual pH and electric potential stimuli. Bohn and coworkers demonstrated pHresponsive, charge-selective ion gating by placing polystyrene-b-poly(4vinylpyridine) (PS-b-P4VP) block copolymer (BCP) membranes on top of nanopore electrode arrays (NEA) to create Potential-Induced Wetting and Dewetting in Hydrophobic Nanochannels.... 9

hierarchically-organized multi-component BCP@NEA architectures [23]. The potentialinduced wetting and dewetting behaviors of BCP@NEAs were investigated under conditions in which the nanocylindrical P4VP domains of the BCP membranes exhibit altered surface energy as a function of potential, pH, and ionic strength, Figure 3B [31]. The N atom on the pendant pyridine enables the P4VP domain of the PS-b-P4VP membrane to exhibit two distinct states in response to pH, i.e., a hydrophobic, charge-neutral, collapsed structure at pH values above the p $K_a$  of the P4VP pyridine moieties, and a hydrophilic, positively charged, swollen structure at pH < p $K_a$ (P4VP). Consequently, the hydrophobic nanochannels prevent water and ions from permeating across the BCP membrane at pH > p $K_a(P4VP)$ , while anionpermselective transport is obtained at pH < p $K_a$ (P4VP). Surprisingly, in the hydrophobic, collapsed, charge-neutral state, the BCP nanochannels can be induced to support transmembrane transport of anions, cations, and neutrals when a sufficiently negative potential is applied across the BCP membrane. This potential-induced wetting, when applied to the BCP@NEA architectures, makes it possible to capture, then trap, redox species under external control, thereby suggesting the use of reversible, potential-induced wetting and dewetting for ultrasensitive chemical sensing. An analyte-containing solution introduced into nanopores via electrowetting can be isolated from the bulk solution by the hydrophobic BCP membrane when the potential bias is released. The redox species, isolated from the background of the remainder of the electrolyte outside the nanopore, can then be detected at enhanced sensitivity by redox cycling-based current amplification.

# Applications based on potential-induced wetting and dewetting

Even though potential (or electric-field)-controlled wettability manipulation holds exceptional promise, only a limited number of examples have been demonstrated to-date. In

particular, applications based on potential-induced wetting and dewetting of hydrophobic nanopores have yet to be reported, principally because fundamental understanding of potential-controlled wettability manipulation in nanoconfined geometries is still being developed; applications will surely follow.

Among the applications explored so far, liquid-liquid separations, such as water-oil and other similar mixtures, offer attractive possibilities. For example, Tuteja and coworkers exploited electrowetting to demonstrate on-demand separation using gravity-driven filtration of water-oil mixtures [51]. Effective oil-water separations were designed based on the opposite electrowetting behaviors of water and oil on dielectric substrates. Upon applying a potential up to 2.0 kV, electrowetting is promoted in water droplets on dielectrics, decreasing the contact angle, while oil droplets exhibit unchanged, or even slightly increased, contact angles. These opposite electrowetting behaviors enable gravity-driven oil/water separations with  $\geq 99.9\%$  separation efficiency when the crude mixture is placed on a textured membrane substrate, consisting of 50 wt% 1H, 1H, 2H, 2H-heptadecafluorodecyl polyhedral oligomeric silsequioxane (fluorodecyl POSS) and PDMS.

Similarly, Oh and coworkers advanced the use of wettability manipulation for electrowetting-mediated active flow control devices utilizing repellency and permeability control on graphene-coated meshes, as shown in **Figure 4A** [52]. However, the use of large potentials to achieve separations has to address the tendency to cause oxidation-derived damage, leading to corrosion. To circumvent this problem, nickel meshes were coated with a few layers of graphene, significantly improving the stability against corrosion. Because graphene is hydrophobic, in the absence of potential water droplets remain on the surface of the mesh at high contact angle, *i.e.*, the surfaces exhibit hydrophobic repellency. However, when a potential is applied between two parallel electrodes, *e.g.*, graphene-coated mesh and

copper, electrowetting of the water droplet at the graphene-coated mesh causes the contact angle to decrease, thus allowing the movement of water droplets through the mesh towards the Cu electrode, achieving transient potential-stimulated liquid permeation.

Early studies demonstrated efficient separation of oil-water mixtures, but the used methods required high voltages or electric fields, e.g., 2.0 kV or 10 kV cm<sup>-1</sup>, to achieve sufficient differential wettability of water and oil to effect workable separations, thus limiting their practical use. In contrast, Jiang and coworkers reported electric-field-controlled wettability switching at more moderate voltages, ~170 V [53]. They fabricated a hierarchically organized micro/nanostructured mesh via emulsion polymerization of aniline on microscale stainless steel mesh. The resulting nanostructured polyaniline-coated mesh is both superhydrophobic and superoleophobic in the absence of applied bias. Upon applying a sufficiently large voltage, a water wettability transition occurs, decreasing the contact angle, and allowing water to permeate the mesh. In contrast, the superoleophobic character of the mesh is maintained, and the wettability of oil is unchanged in the presence of an applied voltage, thus achieving an efficient oil-water separation. More recently, a gated, pulsatile drug delivery system was proposed by Zhai and coworkers [54]. Unlike previous approaches that achieved oil-water separation using the purely physical strategy of electrowetting on dielectric layercoated conductive meshes, this approach used the redox chemistry of polypyrrole (PPy) doped with perfluorooctanesulfonate (PFOS<sup>-</sup>) deposited on nanoporous anodic aluminum oxide to achieve electrically actuated nanochannels for valve-like gated drug delivery, Figure 4B. The PFOS--doped PPy film is hydrophobic at oxidizing potentials, thus producing a gate-closed state. Conversely, poising the electrode at reducing potentials, PFOS<sup>-</sup> is expelled from the PPy film, producing a hydrophilic structure and gate-open response, allowing drug release, as shown in Figure 4C.

### **Conclusions**

In this Current Opinion, we have surveyed recent work focusing on potential- and other stimuli-induced wetting and dewetting behaviors in confined hydrophobic channels. Despite early simulations suggesting that hydrophobic gating in biological channels is a key process controlling rapid ion permeation, reversible wetting and dewetting to manipulate fluidic behavior in synthetic nanochannels was not experimentally realized until the early 2010s. In addition, detailed rigorous understanding of the mechanisms supporting wetting/dewetting behavior in nanoscale hydrophobic channels is only just beginning to emerge. Continued work in this area should establish relationships between the various perturbations, such as ionic strength, nanochannel geometry, e.g., channel shape, diameter, and length, and types of ionic species and transport behavior in these structures. Clearly, these fundamental investigations on controlling wetting and dewetting transitions will ultimately lead to further practical applications in disparate areas such as fluidic valving for drug delivery, oil/water separation, water treatment, and ultrasensitive biosensing. Finally, there are great opportunities in extending electrowetting to the use of additional external perturbations, either singly or in combination, to achieve reversible wetting and dewetting transitions, thereby significantly extending the range and impact of these electrochemical manipulations of molecular transport.

### **Conflict of interest statement**

Nothing declared.

# Acknowledgements

Work from the authors' laboratories described here was supported by the National Science

Foundation through grant 1904196 and the Department of Energy Office of Science through

grant DE FG02 07ER15851, as well as the National Research Foundation of Korea (NRF) grant

funded by the Korea government (MSIT) (No. 2021R1F1A1061261).

# **Author information**

Corresponding Author

\*E-mail: pbohn@nd.edu. Tel.: +1 574 631 1849. Fax: +1 574 631 8366.

14

**ORCID** 

Seol Baek: 0000-0003-2191-6723

Seung-Ryong Kwon: 0000-0002-0890-523X

Paul W. Bohn: 0000-0001-9052-0349

Potential-Induced Wetting and Dewetting in Hydrophobic Nanochannels.....

### References

Papers of particular interest, published within the period of review, have been highlighted as:

- \* of special interest
- \*\* of outstanding interest
- [1] E. Gouaux, R. MacKinnon: Principles of Selective Ion Transport in Channels and Pumps. Science 2005, 310:1461-1465.
- [2] O. Beckstein, M.S.P. Sansom: Liquid-vapor oscillations of water in hydrophobic nanopores. *Proc. Natl. Acad. Sci.* 2003, **100**:7063.
- [3] M.Ø. Jensen, D.W. Borhani, K. Lindorff-Larsen, P. Maragakis, V. Jogini, M.P. Eastwood, R.O. Dror, D.E. Shaw: **Principles of conduction and hydrophobic gating in K**<sup>+</sup> **channels**. *Proc. Natl. Acad. Sci.* 2010, **107**:5833.
- [4] C. Neale, N. Chakrabarti, P. Pomorski, E.F. Pai, R. Pomès: **Hydrophobic Gating of Ion Permeation in Magnesium Channel CorA**. *PLoS Comput. Biol.* 2015, **11**:e1004303.
- \*[5] G. Klesse, S.J. Tucker, M.S.P. Sansom: Electric Field Induced Wetting of a Hydrophobic Gate in a Model Nanopore Based on the 5-HT3 Receptor Channel. *ACS Nano* 2020, **14**:10480-10491.

This paper investigates the transmembrane voltage-controlled hydrophobic gating of a model nanopore, 5-HT<sub>3</sub>, by molecular dynamics simulations, demonstrating a thresold electric field of  $\sim$ 100 mV nm<sup>-1</sup> required for the hydrophobic pore hydration .

- [6] X. Zhang, H. Liu, L. Jiang: Wettability and Applications of Nanochannels. *Adv. Mater.* 2019, **31**:1804508.
- [7] Y. Li, L. He, X. Zhang, N. Zhang, D. Tian: External-Field-Induced Gradient Wetting for Controllable Liquid Transport: From Movement on the Surface to Penetration into the

Surface. Adv. Mater. 2017, 29:1703802.

- [8] M. Nazari, A. Davoodabadi, D. Huang, T. Luo, H. Ghasemi: **Transport Phenomena in Nano/Molecular Confinements**. *ACS Nano* 2020, **14**:16348-16391.
- [9] H. Zhang, Y. Tian, L. Jiang: Fundamental studies and practical applications of bioinspired smart solid-state nanopores and nanochannels. *Nano Today* 2016, 11:61-81.
- [10] M. Pevarnik, W. Cui, S. Yemenicioglu, J. Rofeh, L. Theogarajan: Solid-state nanopore based biomimetic voltage gated ion channels. *Bioinspiration Biomimetics* 2017, 12:066008.
- [11] D. Kaya, K. Keçeci: Review—Track-Etched Nanoporous Polymer Membranes as Sensors: A Review. J. Electrochem. Soc. 2020, 167:037543.
- [12] L.P. Zaino, C. Ma, P.W. Bohn: Nanopore-enabled electrode arrays and ensembles. *Microchim. Acta* 2016, **183**:1019-1032.
- [13] L.P. Zaino III, N.M. Contento, S.P. Branagan, P.W. Bohn: Coupled Electrokinetic Transport and Electron Transfer at Annular Nanoband Electrodes Embedded in Cylindrical Nanopores. ChemElectroChem 2014, 1:1570-1576.
- [14] L.R. Gibson II, S.P. Branagan, P.W. Bohn: Convective Delivery of Electroactive Species to Annular Nanoband Electrodes Embedded in Nanocapillary-Array Membranes. *Small* 2013, 9:90-97.
- [15] S.P. Branagan, N.M. Contento, P.W. Bohn: Enhanced Mass Transport of Electroactive Species to Annular Nanoband Electrodes Embedded in Nanocapillary Array Membranes. *J. Am. Chem. Soc.* 2012, **134**:8617-8624.
- [16] T. Ma, J.-M. Janot, S. Balme: **Track-Etched Nanopore/Membrane: From Fundamental to Applications**. *Small Methods* 2020, 4:2000366.

[17] K. Fu, S.-R. Kwon, D. Han, P.W. Bohn: Single Entity Electrochemistry in Nanopore Electrode Arrays: Ion Transport Meets Electron Transfer in Confined Geometries. *Acc. Chem. Res.* 2020, **53**:719-728.

\*\*[18] M.R. Powell, L. Cleary, M. Davenport, K.J. Shea, Z.S. Siwy: **Electric-field-induced** wetting and dewetting in single hydrophobic nanopores. *Nat. Nanotechnol.* 2011, **6**:798-802.

This work acheives the repetitive wetting and dewetting of single nanopores exhibiting high and zero conductance controlled by electric field.

[19] H. Kwok, K. Briggs, V. Tabard-Cossa: Nanopore Fabrication by Controlled Dielectric Breakdown. PLoS One 2014, 9:e92880.

[20] R.H. Tunuguntla, R.Y. Henley, Y.-C. Yao, T.A. Pham, M. Wanunu, A. Noy: **Enhanced** water permeability and tunable ion selectivity in subnanometer carbon nanotube porins. *Science* 2017, **357**:792-796.

[21] I. Vlassiouk, C.-D. Park, S.A. Vail, D. Gust, S. Smirnov: Control of Nanopore Wetting by a Photochromic Spiropyran: A Light-Controlled Valve and Electrical Switch. *Nano Lett.* 2006, **6**:1013-1017.

[22] Z. Zhang, X.-Y. Kong, K. Xiao, Q. Liu, G. Xie, P. Li, J. Ma, Y. Tian, L. Wen, L. Jiang: Engineered Asymmetric Heterogeneous Membrane: A Concentration-Gradient-Driven Energy Harvesting Device. J. Am. Chem. Soc. 2015, 137:14765-14772.

[23] S. Baek, S.-R. Kwon, K. Fu, P.W. Bohn: Ion Gating in Nanopore Electrode Arrays with Hierarchically Organized pH-Responsive Block Copolymer Membranes. *ACS Appl. Mater. Interfaces* 2020, 12:55116-55124.

[24] C.I. Lynch, S. Rao, M.S.P. Sansom: Water in Nanopores and Biological Channels: A Molecular Simulation Perspective. *Chem. Rev.* 2020, **120**:10298-10335.

[25] P. Aryal, M.S.P. Sansom, S.J. Tucker: **Hydrophobic Gating in Ion Channels**. *J. Mol. Biol.* 2015, **427**:121-130.

[26] U. Rant: Water flow at the flip of a switch. Nat. Nanotechnol. 2011, 6:759-760.

\*\*[27] S.N. Smirnov, I.V. Vlassiouk, N.V. Lavrik: **Voltage-Gated Hydrophobic Nanopores**.

\*\*[27] S.N. Smirnov, I.V. Vlassiouk, N.V. Lavrik: **Voltage-Gated Hydrophobic Nanopores**.

This paper is the first experimental demonstration of voltage-controlled wetting and dewetting in hydrophobic nanopores.

[28] K. Xiao, Y. Zhou, X.-Y. Kong, G. Xie, P. Li, Z. Zhang, L. Wen, L. Jiang: Electrostatic-Charge- and Electric-Field-Induced Smart Gating for Water Transportation. *ACS Nano* 2016, **10**:9703-9709.

\*[29] G. Xie, P. Li, Z. Zhao, Z. Zhu, X.-Y. Kong, Z. Zhang, K. Xiao, L. Wen, L. Jiang: Light-and Electric-Field-Controlled Wetting Behavior in Nanochannels for Regulating Nanoconfined Mass Transport. *J. Am. Chem. Soc.* 2018, **140**:4552-4559.

The authors report dual stimuli (electric field and light)-controlled wetting and dewetting in nanochannels using host-guest chemistry.

\*\*[30] S.-R. Kwon, S. Baek, K. Fu, P.W. Bohn: Electrowetting-Mediated Transport to Produce Electrochemical Transistor Action in Nanopore Electrode Arrays. *Small* 2020, 16:1907249.

This work exploits electric-field-controlled reversible wetting and dewetting for realizing electrochemical transistor action.

\*[31] S.-R. Kwon, S. Baek, Paul W. Bohn: **Potential-induced wetting and dewetting in pH-responsive block copolymer membranes for mass transport control**. *Faraday Discuss*. 2021, https://doi.org/10.1039/D1FD00048A.

The authors demonstrate the isolation and confinement of an electrolyte solution from bulk solution across a pH-responsive block compolymer membrane and into a synthetic nanopore using electrically controllable wetting and dewetting in the hydrophobic block domain.

- [32] B.R.H. de Aquino, H. Ghorbanfekr-Kalashami, M. Neek-Amal, F.M. Peeters: **Ionized** water confined in graphene nanochannels. *Phys. Chem. Chem. Phys.* 2019, **21**:9285-9295.
- [33] K.-i. Otake, K. Otsubo, T. Komatsu, S. Dekura, J.M. Taylor, R. Ikeda, K. Sugimoto, A. Fujiwara, C.-P. Chou, A.W. Sakti, Y. Nishimura, H. Nakai, H. Kitagawa: Confined water-mediated high proton conduction in hydrophobic channel of a synthetic nanotube. *Nat. Commun.* 2020, 11:843.
- [34] H. Zhu, Y. Wang, Y. Fan, J. Xu, C. Yang: Structure and Transport Properties of Water and Hydrated Ions in Nano-Confined Channels. *Adv. Theory Simul.* 2019, **2**:1900016.
- [35] P. Ball: Water is an active matrix of life for cell and molecular biology. *Proc. Natl. Acad. Sci.* 2017, **114**:13327.
- [36] G. Hummer, J.C. Rasaiah, J.P. Noworyta: Water conduction through the hydrophobic channel of a carbon nanotube. *Nature* 2001, 414:188-190.
- [37] L. Hua, R. Zangi, B.J. Berne: Hydrophobic Interactions and Dewetting between Plates with Hydrophobic and Hydrophilic Domains. *J. Phys. Chem. C* 2009, **113**:5244-5253.
- [38] A.J. Patel, P. Varilly, S.N. Jamadagni, M.F. Hagan, D. Chandler, S. Garde: Sitting at the Edge: How Biomolecules use Hydrophobicity to Tune Their Interactions and Function. *J.*

- Phys. Chem. B 2012, 116:2498-2503.
- [39] Z. Jia, M. Yazdani, G. Zhang, J. Cui, J. Chen: **Hydrophobic gating in BK channels**. *Nat. Commun.* 2018, **9**:3408.
- [40] M.A. Kasimova, A. Yazici, Y. Yudin, D. Granata, M.L. Klein, T. Rohacs, V. Carnevale: Ion Channel Sensing: Are Fluctuations the Crux of the Matter? *J. Phys. Chem. Lett.* 2018, 9:1260-1264.
- [41] G. Klesse, S. Rao, M.S.P. Sansom, S.J. Tucker: **CHAP: A Versatile Tool for the Structural and Functional Annotation of Ion Channel Pores**. *J. Mol. Biol.* 2019, **431**:3353-3365.
- [42] S. Rao, G. Klesse, P.J. Stansfeld, S.J. Tucker, M.S.P. Sansom: A heuristic derived from analysis of the ion channel structural proteome permits the rapid identification of hydrophobic gates. *Proc. Natl. Acad. Sci.* 2019, **116**:13989.
- [43] S. Rao, C.I. Lynch, G. Klesse, G.E. Oakley, P.J. Stansfeld, S.J. Tucker, M.S.P. Sansom: Water and hydrophobic gates in ion channels and nanopores. *Faraday Discuss*. 2018, 209:231-247.
- [44] C.D. Daub, D. Bratko, K. Leung, A. Luzar: Electrowetting at the Nanoscale. *J. Phys. Chem. C* 2007, 111:505-509.
- [45] F.H. Song, B.Q. Li, C. Liu: Molecular Dynamics Simulation of Nanosized Water Droplet Spreading in an Electric Field. *Langmuir* 2013, **29**:4266-4274.
- [46] J.L. Trick, C. Song, E.J. Wallace, M.S.P. Sansom: Voltage Gating of a Biomimetic Nanopore: Electrowetting of a Hydrophobic Barrier. *ACS Nano* 2017, **11**:1840-1847.
- [47] A.T. Celebi, M. Barisik, A. Beskok: Electric field controlled transport of water in

graphene nano-channels. J. Chem. Phys. 2017, 147:164311.

[48] L. Innes, D. Gutierrez, W. Mann, S.F. Buchsbaum, Z.S. Siwy: **Presence of electrolyte** promotes wetting and hydrophobic gating in nanopores with residual surface charges. *Analyst* 2015, **140**:4804-4812.

[49] J. Sheng, Q. Zhu, X. Zeng, Z. Yang, X. Zhang: Promotion of Water Channels for Enhanced Ion Transport in 14 nm Diameter Carbon Nanotubes. ACS Appl. Mater. Interfaces 2017, 9:11009-11015.

\*\*[50] J.W. Polster, E.T. Acar, F. Aydin, C. Zhan, T.A. Pham, Z.S. Siwy: **Gating of Hydrophobic Nanopores with Large Anions**. *ACS Nano* 2020, **14**:4306-4315.

This paper shows that the transport of aqueous solutions through nanopores containing a hydrophobic-hydrophilic juction depends on the type of ions as well as the application of an electric field.

[51] G. Kwon, A.K. Kota, Y. Li, A. Sohani, J.M. Mabry, A. Tuteja: **On-Demand Separation** of Oil-Water Mixtures. *Adv. Mater.* 2012, **24**:3666-3671.

[52] R. Tabassian, J.-H. Oh, S. Kim, D. Kim, S. Ryu, S.-M. Cho, N. Koratkar, I.-K. Oh: Graphene-coated meshes for electroactive flow control devices utilizing two antagonistic functions of repellency and permeability. *Nat. Commun.* 2016, 7:13345.

[53] X. Zheng, Z. Guo, D. Tian, X. Zhang, L. Jiang: Electric Field Induced Switchable Wettability to Water on the Polyaniline Membrane and Oil/Water Separation. *Adv. Mater. Interfaces* 2016, **3**:1600461.

\*\*[54] Q. Zhang, J. Kang, Z. Xie, X. Diao, Z. Liu, J. Zhai: Highly Efficient Gating of Electrically Actuated Nanochannels for Pulsatile Drug Delivery Stemming from a

Reversible Wettability Switch. Adv. Mater. 2018, 30:1703323.

This work utilizes an elecro-actuated wettability switch though nanochannels as a transport valve for highly efficient pulsatile drug delivery.

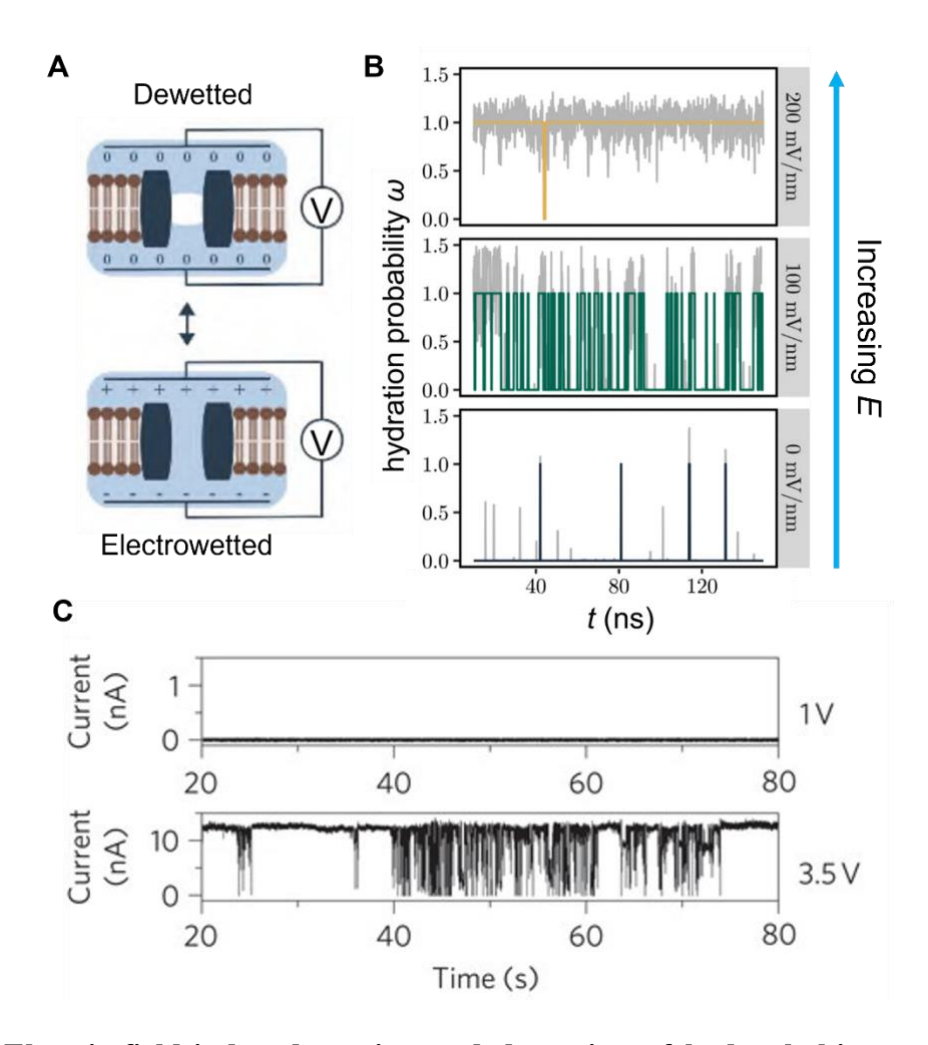
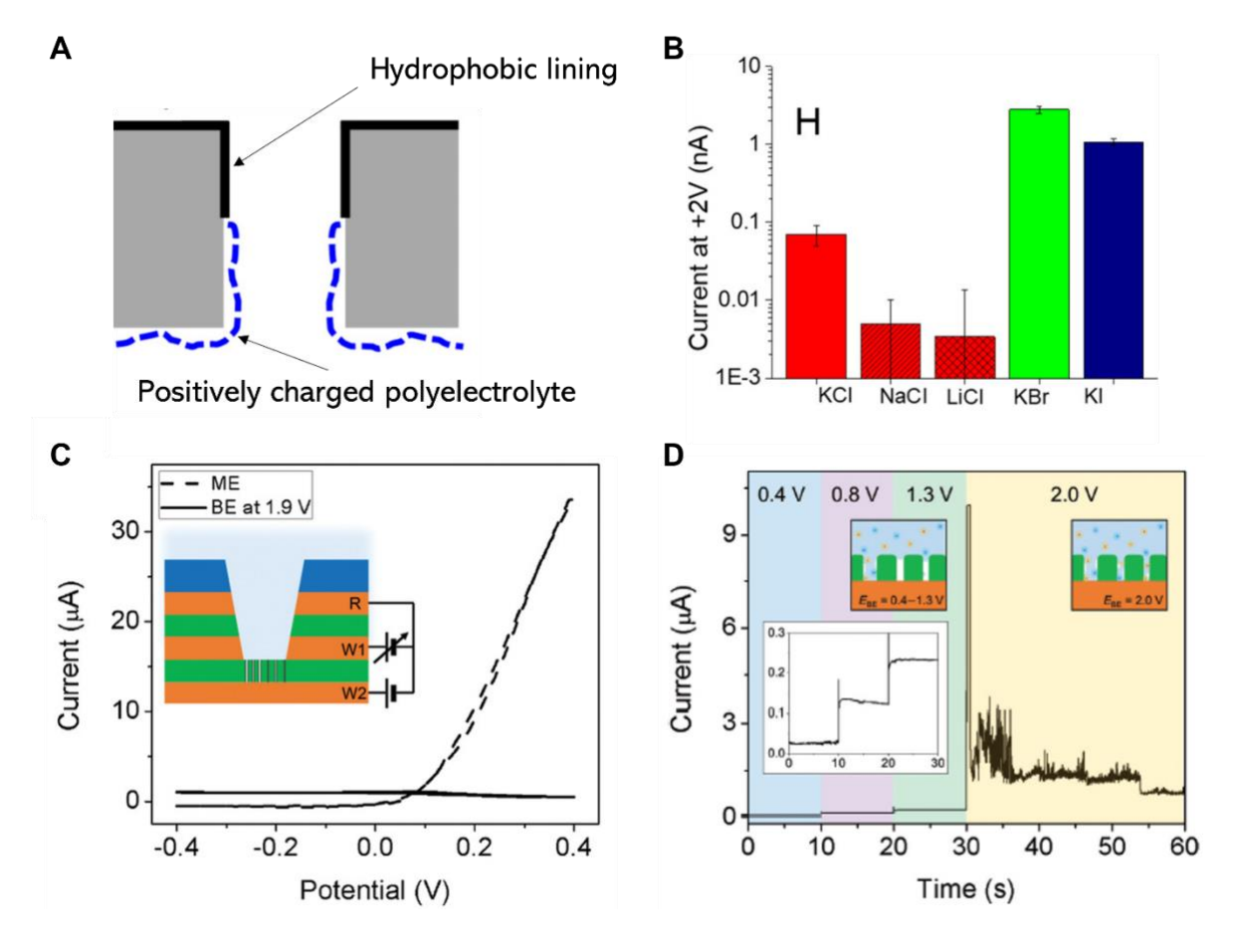


Figure 1. Electric-field-induced wetting and dewetting of hydrophobic nanopores. A.

Schematic illustration of the liquid-to-vapor transition associated with potential-controlled wetting and dewetting, respectively. **B**. Time-dependent hydration probability ( $\omega$ ) in the M2 helix nanopore at different trans-electric-field strengths from 0 to 200 mV/nm. The grey background lines denote the normalized minimum water density with respect to bulk water. The colored (yellow, green, and black) lines denote discretization through a threshold algorithm determining for closed and open states, *i.e.*,  $\omega(t) = 0$  or 1, respectively. Reproduced with permission from ref [5]. **C**. Current-time response of single hydrophobic nanopores exhibiting zero (dewetted) and high (wetted) conductance at  $E_{appl} = 1$  V and 3.5 V, respectively. Reproduced with permission from ref [18].



**Figure 2. A.** Single nanopore containing a hydrophilic-hydrophobic juction. **B.** Ionic current at  $E_{appl} = +2$  V obtained with diffferent electroyte species. Reproduced with permission from ref [50]. Copyright 2020 American Chemical Society. **C.** Electrowetting-mediated electrochemical transistor operation, in which the bottom electrode (W2) was held at  $E_{appl} = +1.9$  V, while the middle electrode (W1) was swept in the potential range -0.4 V  $< E_{appl} < +0.4$  V with respect to the top reference electrode (R). **D.** Current-time measurements at increasing potential steps from +0.4 to +2.0 V at the bottom electrode relative to the top electrode. At a bottom electrode potential  $E_{BE} = +2.0$  V, strong current fluctuations are observed with the interpretation of defect electrowetting in SiN<sub>x</sub> nanochannels. Reprinted with permission from ref [23].

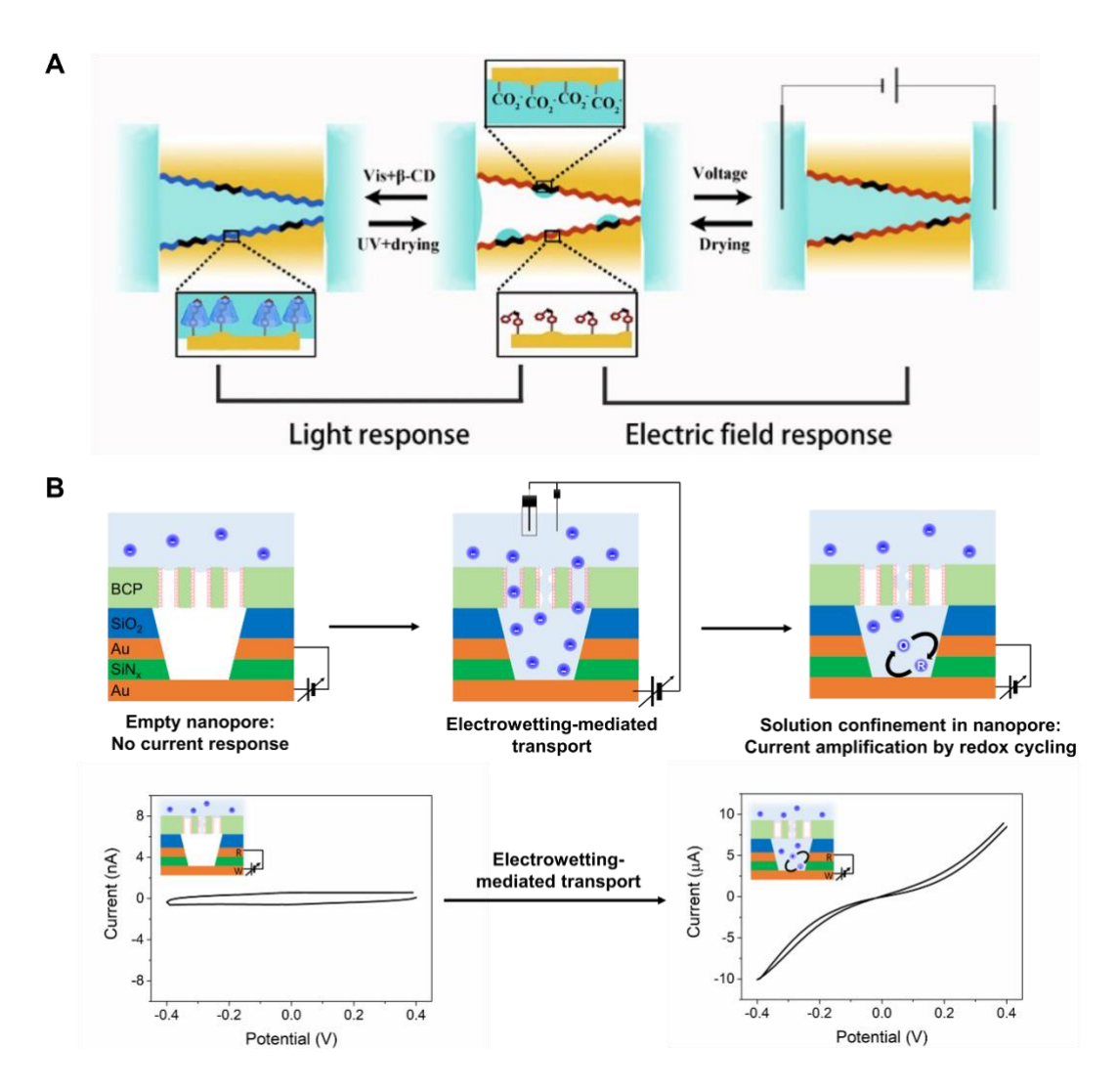
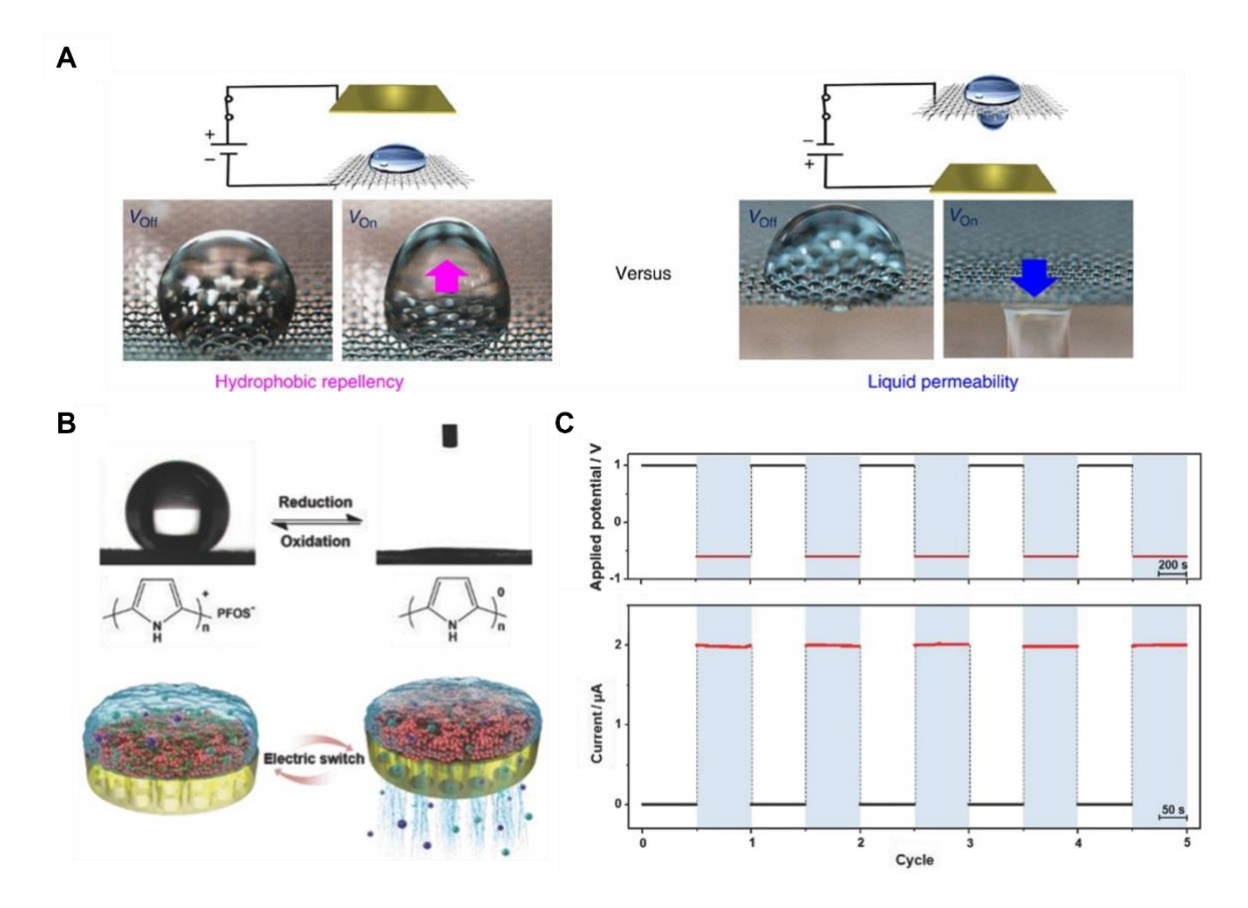


Figure 3. Multiple external stimuli-controlled wetting and dewetting of nanochannels. A.

Schematic illustration of light- and electric-field-controlled wettability in Azo-modified nanochannels. Hydrophobic nanochannels in the dewetted state (*middle*) switch to the wetted state by light-responsive host-guest reaction between Azo and  $\beta$ -cyclodextrins (*left*) or electrowetting (*right*). Reprinted with permission from ref [29]. Copyright 2018 American Chemical Society. **B**. Schematic illustration of electrowetting-mediated transport in hierarchically organized PS-*b*-P4VP BCP@NEAs at pH > p $K_a$ (P4VP). Hydrophobic BCP channels initially block water/ion transport (*upper left*). Application of a sufficiently large bias voltage causes potential-induced wetting, the channels temporarily open and solution species can be transported in the interior of the nanopores (*upper middle*). Subsequently, if the potential

is relaxed, the BCP nanochannels can be dewetted, trapping solution species in the interior of the NEA nanopores, followed by redox cycling-based electrochemical detection (*upper right*). (*Lower*) Voltametric responses of 50 mM Fe(CN) $_6$ <sup>3/4-</sup> at pH 7.6 were obtained before and after potential-induced wetting enabled solution to be introduced into the nanopores presenting a 2-electrode configuration using bottom and top electrodes as working and counter electrodes, respectively. Reprinted with permission from ref [31].



**Figure 4.** Applications based on potential-induced wetting and dewetting. **A.** Schematic diagrams and photographs illustrating electrowetting of graphene-coated nickel meshes for functionally antagonistic flow control utilizing hydrophobic repellency and liquid permeability controlled by electric stimuli. Reprinted with permission from ref [52]. **B.** Electrically actuated gating in a PFOS<sup>-</sup>-doped PPy film on AAO membrane. Reversible wettability of the PPy switches between superhydrophobic (*left*) and superhydrophilic (*right*) states in response to redox potnetials. **C.** Typical ionic current response to the alternating application of oxidizing (+1 V) and reducing (-1 V) potentials (*vs.* Ag/AgCl) applied to the PPy film of nanochannels using 1 mM KCl solution at pH 6.1. Reproduced with permission from ref [54].